Colloidal interactions mediated via polyelectrolytes

Rudolf Podgornik[a)]
Division of Computer Research & Technology, National Institutes of Health, Bethesda, MD 20892

Torbjörn Åkesson and Bo Jönsson
Physical Chemistry 2, Chemical Center, P.O. Box 124, S - 221 00 Lund, Sweden

(Received 28 March 1994; accepted 7 March 1995)

Using Monte Carlo simulation, scaling, variational and mean-field arguments we investigate forces between charged spherical aggregates conferred by oppositely charged polymeric chains. Two types of polymer mediated attraction are found in this system, both of a bridging type but differing markedly in terms of the range. The *entropic* bridging force is of a range comparable to the average monomer–monomer separation in the chain. It is present whenever many chains have to compensate the charge on two macroions. The *energetic* bridging force has a range of the order of the length of the polymer chain and pertains to situations when a single chain has to compensate the charge on more than one macroion. In what follows we shall give a detailed analysis of both bridging interactions with a special regard for polycounterion versus simple counterion effects. The two types of bridging are in a certain sense complementary and should be present in polymer– surfactant systems at different regimes of the polymer–macroion concentration ratios. © *1995 American Institute of Physics.*

I. INTRODUCTION

The interaction between two macroions immersed in an electrolyte solution is normally dominated by strong repulsive forces. The repulsion has its origin in the overlap of the diffuse double layers of counterions neutralizing the charged particles.[1] The interaction is well described by mean-field theory as long as the counterions are monovalent. The mean-field theory neglects correlations between the counterions and as a consequence there is an attractive force component lacking in it.[2] The attractive component turns out to be the dominating one in many systems with divalent counterions, or elsewhere when the ion–ion interaction is strong. This has been clearly shown in simulations and anisotropic hypernetted chain calculations.[2,3]

Addition of neutral salt to an electric double layer normally leads to a decreased repulsion, that is, the macroion–macroion interaction becomes screened. The screening is exponential and the mean-field approach works very well for a 1:1 salt, as demonstrated by comparison with surface force experiments.[4] In a double layer with divalent counterions or where the added salt contains divalent counterions the outcome is less clear. We can, for example, envisage a situation where the original repulsive interaction turns attractive, but also the opposite should be possible. The situation for divalent counterions can be summarized as a delicate balance between attractive and repulsive forces with a generally very weak *net* force. The ionic size will only be important at very short separations and will therefore further complicate the picture, but we will leave this morass and instead turn to polyelectrolyte counterions.

Polyelectrolytes are quite common in colloidal systems both in nature and in technological applications and what makes this study worthwhile is that they have a profound influence on the colloid stability.[5] Let us recapitulate the behavior in a salt-free system, where polyelectrolytes act as counterions to two infinite charged planar walls. The two uniformly charged walls are neutralized by polyelectrolytes consisting of monomers of the opposite charge. The chains are free to move in the intervening space and the monomer–monomer bonds are described as simple harmonic potentials with zero equilibrium separation. The repulsive double layer interaction seen with monovalent counterions will completely disappear under these conditions and the polyelectrolytes will instead give rise to a strong short ranged attraction.[6] The attraction is due to chains bridging from one charged wall to the other. This means that the attraction stems from an elastic stretching of the chains. The electrostatic repulsion between the chains forces them to reside close to the charged walls—this is the energetically most favorable configuration. The chain entropy, however, is very low under these conditions. Thus, by bridging from one charged wall to the other one, the chain gains substantial entropy. The electrostatic potential is very high in the midregion, which means that the bridging can only involve one or two monomers. The attraction will be strong, but short ranged and of importance only when the surface–surface separation is of the same order as the monomer–monomer separation. For separations larger than the monomer–monomer distance the interaction will be virtually zero and much smaller than the ordinary double-layer repulsion, hence not detectable by a surface force experiment.[7]

The chain length has only a marginal influence on the attraction, since the bridging only involves one or two bonds. Whether the chains are free or grafted with one end to either of the two walls is immaterial as is also the detailed description of the bonding potential between the monomers of the chain.[8] The attraction will increase with surface charge density, the minimum in the force-distance curve will become deeper and more narrow at the same time as it is shifted inwards. This behavior is qualitatively described in the polyelectrolyte mean-field theory due to Podgornik.[9]

[a)]On leave from J.Stefan Institute, P.O.B. 100, 61000 Ljubljana, Slovenia.

The assumption of perfect matching between the amount of charge on the walls and on the polyelectrolyte is of course a highly idealized situation and under most experimental situations one will find either an over- or undercompensated system. The conclusions stated above will remain valid if there is a small imbalance in charge, but a strongly over- or undercompensated system will not show any attractive interaction.[7]

The case of interacting spherical aggregates in the presence of polycounterions differs from the interaction between two infinitely extended planar surfaces mainly in the fact that the polyelectrolyte counterions are not only subjected to electrostatic self-interactions but are also in a large attractive electrostatic field provided by the two oppositely charged macroions. As is known there is no corresponding electrostatic field between two infinite equally charged planar surfaces. One would thus expect that if anything the bridging attraction between charged aggregates of finite extension should be even more pronounced. We will thus try to establish the details of this bridging attraction between two spherical macroions under different conditions.

There are also clear experimental indications that polyelectrolyte promoted bridging is particularly relevant in the case of interaction between polyelectrolytes and ionic micelles or silicic acid colloid particles.[10] The existence of electrostatically bound polyelectrolyte–colloid particle complexes has been inferred, composed of a single polyelectrolyte chain with at least two and up to several tens of colloid particles. The polymer–micelle complex in the latter case resembles a necklace of up to 30 micelles threaded along the polymer chain.[11] Furthermore the interaction between DNA and cationic liposomes starts with the bridging induced complexation of liposomes[12] that later leads to encapsulation of DNA and its eventual transfection in the presence of cells, a process of considerable practical significance but unfortunately still poorly understood.

In what follows we shall investigate the interaction between two charged spherical aggregates mediated by neutralizing polyelectrolyte chains. We shall analyze the effect of simple- and polycounterions on the net force between the aggregates. The result of our computation, which is within the framework set by the spherical *cell model*,[13] is a mean force between spherical aggregates. We thus disregard all many-body effects that should be of some importance in this system but are on the other hand extremely difficult to analyze. The difficulties stem mainly from the pronounced charge dissymmetry of the system that contains highly charged macroions and polycounterions together with simple ions. This leads to configurations of tight association between macroions and polycounterions, thus making independent trial Monte Carlo moves of the macroions difficult to find. By avoiding these difficulties through the use of the *cell model* we have admittedly simplified the system but we believe the simplifications are more than compensated by the insight that one can thus gain into the effective macroion pair interaction. A short version of this work was published in Ref. 14.

II. MICROSCOPIC MODEL

The model system composed of a polyelectrolyte chain N monomers long, two macroions at $\mathbf{R}_1$ and $\mathbf{R}_2$, and N_C simple counterions, is described with the following model (effective) Hamiltonian:

$$\begin{aligned}\mathscr{H}(N)=&\sum_{i=1}^{N-1} u_B[|\mathbf{r}(i)-\mathbf{r}(i+1)|]+\frac{1}{2}\sum_{i,j=1}^{N+N_C} u_C[|\mathbf{r}(i)-\mathbf{r}(j)|]\\&+\sum_{i=1}^{N+N_C}\{\mathscr{U}_C[|\mathbf{R}_1-\mathbf{r}(i)|]+\mathscr{U}_C[|\mathbf{R}_2-\mathbf{r}(i)|]\}\\&+\mathscr{U}_C(|\mathbf{R}_2-\mathbf{R}_1|)+\frac{1}{2}\sum_{i,j=1}^{N+N_C} u_{\mathrm{HC}}[|\mathbf{r}(i)-\mathbf{r}(j)|]\\&+\sum_{i=1}^{N+N_C}\{\mathscr{U}_{\mathrm{HC}}[|\mathbf{R}_1-\mathbf{r}(i)|]+\mathscr{U}_{\mathrm{HC}}[|\mathbf{R}_2-\mathbf{r}(i)|]\}.\end{aligned} \tag{2.1}$$

The monomer–monomer bond potential is given by

$$u_B(|\mathbf{r}-\mathbf{r}'|)=\tfrac{1}{2}\mathscr{K}_F|\mathbf{r}-\mathbf{r}'|^2, \tag{2.2}$$

where $\mathscr{K}_F$ is the harmonic force constant characterizing the stiffness of the bond. This is the simplest one parametric model bond potential that one can think of. More complicated expressions introduce additional unknown parameters,[15] a situation that we would definitively like to avoid. Since we want to elucidate qualitative features of the polyelectrolyte behavior the details of the bonding potential are not important.

Furthermore $u_C(|\mathbf{r}-\mathbf{r}'|)$ is the Coulomb interaction potential between two monomers and/or simple counterions both of charge e_0 at $\mathbf{r}$ and $\mathbf{r}'$,

$$u_C(|\mathbf{r}-\mathbf{r}'|)=\frac{e_0^2}{4\pi\epsilon\epsilon_0}\frac{1}{|\mathbf{r}-\mathbf{r}'|}, \tag{2.3}$$

where ϵ and ϵ_0 are the dielectric permittivity of the aqueous medium and the electric constant. $\mathscr{U}_C(|\mathbf{R}-\mathbf{r}|)$ is the Coulomb potential between a macroion of total charge $-e$ located at $\mathbf{R}$ and a monomer or a simple counterion with an elementary charge e_0 at $\mathbf{r}'$:

$$\mathscr{U}_C(|\mathbf{R}-\mathbf{r}'|)=-\frac{ee_0}{4\pi\epsilon\epsilon_0}\frac{1}{|\mathbf{R}-\mathbf{r}'|}. \tag{2.4}$$

Also, $\mathscr{U}_C(|\mathbf{R}-\mathbf{R}'|)$ is a direct Coulomb interaction between two macroions at $\mathbf{R}$ and $\mathbf{R}'$ with a charge $-e$ each.

Instead of using $\mathscr{K}_F$ as a measure of the stiffness of the bond, we can equivalently use a related quantity, $R_{\min}$, which is obtained from the minimization of interaction energy between two monomers, i.e., $R_{\min}=(e_0^2/4\pi\epsilon\epsilon_0\mathscr{K}_F)^{1/3}$ as the parameter describing the strength of the bonds.

The hard-core potentials act either between mobile species (polymer beads and simple counterions)

$$u_{\mathrm{HC}}(|\mathbf{r}-\mathbf{r}'|)=\begin{cases}0, & |\mathbf{r}-\mathbf{r}'|>2d\\ \infty, & |\mathbf{r}-\mathbf{r}'|<2d,\end{cases} \tag{2.5}$$

where $d=2.1$ Å is the hard-core radius of monomers and simple counterions, or between mobile species and the two macroions

$$\mathscr{U}_{\rm HC}(|\mathbf{r}-\mathbf{r}'|)=\begin{cases}0, & |\mathbf{r}-\mathbf{r}'|>R_A+d\\ \infty, & |\mathbf{r}-\mathbf{r}'|<R_A+d,\end{cases} \tag{2.6}$$

where R_A is the hard-core radius of the macroions. The hard-core repulsion between macroions need not be included as they are kept fixed at $\mathbf{R}$ and $\mathbf{R}'$.

The above model is now used as a basis for MC simulations with a fixed value of $R_{\rm min}=6$ Å, $\epsilon=78.3$ and $T=298$ K. In different simulations we vary N, N_C, e, R_A, and $D=|\mathbf{R}_1-\mathbf{R}_2|-2R_A$.

III. BALANCE OF FORCES

The balance of forces in a statistical mechanical ensemble, acting between parts of the system or between the system as a whole and its surroundings can be assesed in a variety of different ways of which the s.c. contact theorem has proved to be most suitable for Monte Carlo applications.[16] This is due to the fact that it contains only statistical averages of mechanical quantities and different moments of density distributions of particles. In a system like the one treated here, the most straightforward expression for the forces acting between two aggregates can be derived from the expression for the average force in a fluid across a fictitious plane, which is conveniently placed at the midpoint between the two macroions.[17] In this way we obtain for the force (F_n) acting along the radius vector joining the two aggregates:

$$F_n=kT\int_{(S)}d^2\mathbf{r}\,\overset{(1)}{\rho}(\mathbf{r})+\int_{(V_1)}\int_{(V_2)}d^3\mathbf{r}_1\,d^3\mathbf{r}_2\,\overset{(2)}{\rho}(\mathbf{r}_1,\mathbf{r}_2)\times\mathbf{f}_n(\mathbf{r}_1,\mathbf{r}_2). \tag{3.1}$$

The subvolumes V_1 and V_2 extend over the left and the right halves of the system so that S coincides with the midplane. $\mathbf{f}_n(\mathbf{r}_1,\mathbf{r}_2)$ is the microscopic force acting between a particle at $\mathbf{r}_1$ and the one at $\mathbf{r}_2$ in the direction of the normal to the dividing surface S between V_1 and V_2. $\overset{(1)}{\rho}(\mathbf{r})$ and $\overset{(2)}{\rho}(\mathbf{r}_1,\mathbf{r}_2)$ are the one and two particle densities. One can show that this expression for the force is closely related to the contact theorem in planparallel geometry.[18]

The first term of Eq. (3.1) is just the momentum exchange between V_1 and V_2 due to the movement of particles across the midplane. It has the form of an ideal osmotic pressure. For the system composed of polycounterions and charged spherical aggregates providing the external electrostatic attraction, the microscopic force $\mathbf{f}_n(\mathbf{r}_1,\mathbf{r}_2)$ is composed of several contributions:[8] the electrostatic force between the polymer beads, the electrostatic force between the polymer beads and the two macroions, the configurational elastic force of the polymer beads whose joining vector passes across S and the contribution of hard-core collisions between mobile particles across S. In this way we obtain for the total force,

$$F_n=F_n(\text{osm})+F_n(\text{cor})+F_n(\text{dir})+F_n(\text{bri})+F_n(\text{col}), \tag{3.2}$$

where osm stands for the osmotic (ideal) momentum exchange contribution, cor for the electrostatic correlation contribution, dir for the direct Coulomb interaction between the two spherical aggregates, and bri the bridging contribution stemming from the stretching of the polymer bonds across the dividing plane and col the collision contribution due to the hard-core part of the interaction potential. The formal definitions of the different force contributions can be written as

$$\begin{aligned}
F_n(\text{osm})&=kT\int_{(S)}d^2\mathbf{r}\,\overset{(1)}{\rho}(\mathbf{r}),\\
F_n(\text{cor})&=-\int_{(V_1)}\int_{(V_2)}d^3\mathbf{r}_1\,d^3\mathbf{r}_2\,\overset{(2)}{\rho}(\mathbf{r}_1,\mathbf{r}_2)\frac{\partial u_C(|\mathbf{r}_1-\mathbf{r}_2|)}{\partial z}\\
&\quad-\int_{(V_1)}d^3\mathbf{r}_1\,\overset{(1)}{\rho}(\mathbf{r}_1)\frac{\partial \mathscr{U}_C(|\mathbf{R}_2-\mathbf{r}_1|)}{\partial z}\\
&\quad-\int_{(V_2)}d^3\mathbf{r}_2\,\overset{(1)}{\rho}(\mathbf{r}_2)\frac{\partial \mathscr{U}_C(|\mathbf{R}_1-\mathbf{r}_2|)}{\partial z},\\
F_n(\text{dir})&=-\frac{\partial \mathscr{U}_C(|\mathbf{R}_1-\mathbf{R}_2|)}{\partial z},\\
F_n(\text{bri})&=-\int_{(V_1)}\int_{(V_2)}d^3\mathbf{r}_1\,d^3\mathbf{r}_2\,\overset{(2)}{\rho}(\mathbf{r}_1,\mathbf{r}_2)\frac{\partial u_B(|\mathbf{r}_1-\mathbf{r}_2|)}{\partial z},\\
F_n(\text{col})&=-\int_{(V_1)}\int_{(V_2)}d^3\mathbf{r}_1\,d^3\mathbf{r}_2\,\overset{(2)}{\rho}(\mathbf{r}_1,\mathbf{r}_2)\frac{\partial u_{\rm HC}(|\mathbf{r}_1-\mathbf{r}_2|)}{\partial z}\\
&=-\int_{(V_1)}\int_{(V_2)}d^3\mathbf{r}_1\,d^3\mathbf{r}_2\,\overset{(2)}{\rho}(\mathbf{r}_1,\mathbf{r}_2)\\
&\quad\times\frac{\partial u_{\rm HC}(r)}{\partial r}\bigg|_{r=|\mathbf{r}_1-\mathbf{r}_2|}\cos\Theta_{1,2}.
\end{aligned} \tag{3.3}$$

$\cos\Theta_{1,2}=z_1-z_2/|\mathbf{r}_1-\mathbf{r}_2|$ is the angle between the normal to the dividing surface S and the direction of the radius vector joining the two colliding particles. In the model of Eq. (2.1) the bonding potential is harmonic thus leading to

$$F_n(\text{bri})=-\mathscr{K}_F\langle|z_i-z_{i+1}|\rangle\times n_{\rm br}, \tag{3.4}$$

where z_i, z_{i+1} are z coordinates (normal to S) of two neighboring beads along the chain that are on the opposite sides of S and $n_{\rm br}$ is the average number of bridges.[8] We now use the standard arguments to convert $\partial u_{\rm HC}(|\mathbf{r}_1-\mathbf{r}_2|)/\partial r$ into a delta function centered on the hard core of the particle, thus obtaining a simplified form of the collision force:[19]

$$F_n(\text{col})=kT\langle\delta(|\mathbf{r}_1-\mathbf{r}_2|-2d)\cos\Theta_{1,2}\rangle, \tag{3.5}$$

where the averaging is done over the distribution of particles in V_1 and V_2.

The above expression for the total force between two subvolumes of the system can be straightforwardly applied to the case of two macroions plus polyelectrolyte (and/or simple counterions) in an infinite volume. If we confine the system to a spherical simulation cell, however, then Eq. (3.1) should also contain an isotropic component of the force, which is not connected with the net interaction between the aggregates at $\mathbf{R}_1$ and $\mathbf{R}_2$, but is rather due to the momentum

exchange at the cell surface. This isotropic component of the force simply reflects the existence of the ''bulk'' isotropic pressure p_{cell} in the system

$$p_{\text{cell}} = kT\rho^{(1)}(R_{\text{cell}}), \tag{3.6}$$

given by the standard contact theorem applicable to hard surfaces.[18] To get the net force between the aggregates we have to subtract this isotropic force contribution

$$F_{\text{cell}} = \int_{(\mathscr{S})} d^2\mathbf{r}\, p_{\text{cell}} \tag{3.7}$$

from F_n in Eq. (3.2), where $\mathscr{S}$ is the area of the cell boundary. The resulting force is the physical net force acting between the macroions, its osmotic contribution being simply rescaled according to

$$F_n(\text{osm}) \to kT \int_{(S)} d^2\mathbf{r}\, \rho^{(1)}(\mathbf{r}) - F_{\text{cell}}, \tag{3.8}$$

where the surface of integration S is the bounding surface between volumes V_1 and V_2 in the simulation cell.

IV. MONTE CARLO SIMULATION TECHNIQUES

Monte Carlo simulations of the system described by the model Hamiltonian [Eq. (2.1)] were performed in a canonical ensemble with the standard Metropolis algorithm.[20] The mobile charges (polymer chains and simple counterions) and the two immobile macroions, see Fig. 1, were enclosed in a spherical simulation cell of radius R_{cell}. Convergence of the force between the two macroions, being the slowest of all the monitored quantities, was used to assess the overall convergence of each simulation. Usually the equilibration runs consisted of approx. $\sim 10^6$ configurations per particle, followed by at least as many configurations in the production run. Each trial move consisted of a random displacement of a randomly chosen monomer or simple counterion on the interval $[-6\ \text{Å}, +6\ \text{Å}]$ in each of the Cartesian directions or equivalently the interval was chosen so that the acceptance rate was between 40%−50%. The main source of rejected configurations was the hard-core monomer (counterion)–macroion interaction.

The most critical simulations are the ones where the chain goes from a captured to a localized state (see below). This region was studied by extra long simulations with 10^7 configurations/particle and in one instance (chain composed of 30 monomers plus 60 additional simple counterions) with 10^8 configurations/particle. The results showed no significant deviations from the shorter simulations with 10^6 configurations/particle.

Three different initial conditions for the positions of the monomers and counterions were tried:

(i) monomers were grouped on the symmetry plane between the two macroions,

(ii) monomers were grouped on the plane behind one of the macroions at the same distance from that macroion as the separation between the macroions, and

(iii) monomers were simply randomly distributed over the simulation cell.

Since no significant differences were detected in the final distributions after the equilibration run of the same length (usually 10^6 configurations/particle, with test cases of up to 10^8 configurations/particle), all of the described simulations used the latter (random) initial condition.

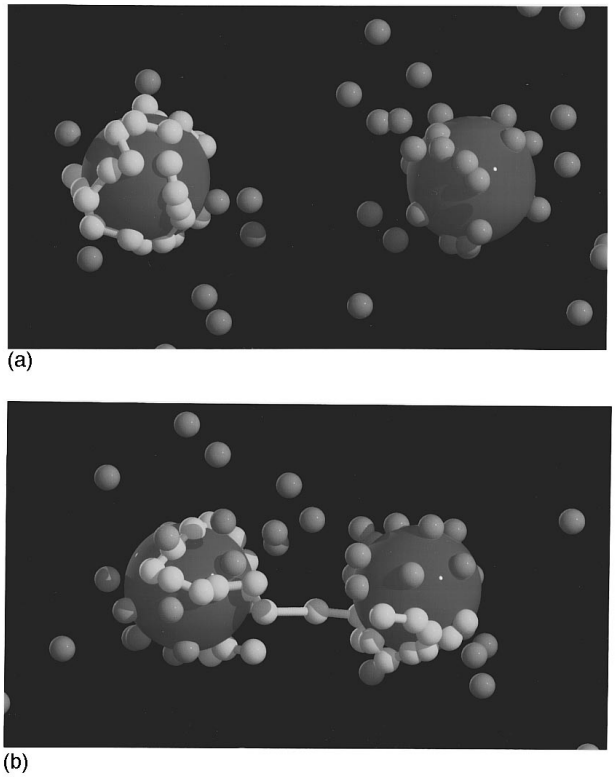

FIG. 1. A simulation snapshot for two different values of the separation between macroions. There are 30 monomers in the chain plus 90 simple counterions in the simulation cell. The upper picture ($D = 60$ Å) presents a *localized* chain and the lower one ($D = 30$ Å) a *captured* chain (see the main text).

The maximum number of mobile charges in the simulations was 120. In this case the equilibration run consisted of 120×10^6 configurations with just as many in the production run. We monitored convergence of the different parts of the conformational energy [Eq. (2.1)], mean end to end separation, radius of gyration, density of the mobile charges at the simulation cell wall, and different components of the force. In **all** of the production runs the accuracy was always better than 10% and was typically around several %. An example of the relative errors in different simulated quantities is given in Table I.

Because of tight complexation between polyelectrolyte chains and oppositely charged macroions when there are no additional simple counterions involved, the isotropic contribution to the interaction force was negligible if simple counterions were not present in the simulation cell. We thus state the values of the simulation cell radius only when simple counterions are present.

The collision contribution to the total force [Eq. (3.5)] could be obtained most accurately through the application of the modified Widom insertion technique.[21] However in the case of connected particles, i.e., polymer chains, we avoided

TABLE I. Average error in different simulated quantities. We chose an example where the approach to equilibrium was slowest and the error largest of all the simulations cited. We use the case of one chain with 30 monomers and 60 counterions. The charge on the macroions just counters the charges of the monomers and the counterions. The hard core diameter was taken as 4.2 Å and the macroion has a diameter of 20 Å. The center to center separation between the macroions is 100.0 Å. The radius of the simulation cell was taken to be 140.00 Å and $R_{\min}$ was 6 Å. The simulation consisted of $\approx 1\times 10^7$ configurations. The definitions of the quantities in the table is given in Sec. III, except for the rms dimensions which are defined in a standard manner (Ref. 28) and the Gaussian energy, which is the energy of all the harmonic bonds.

Quantity	Units	Average value	Error
Coulomb energy	kJ/mol	-0.193×10^4	1%
Gaussian energy	kJ/mol	0.129×10^3	1%
rms radius of gyration	Å	0.225×10^2	2%
rms end–end distance	Å	0.351×10^2	2%
The bridging force	10^{-12} N	-0.207×10^{-3}	2%
The correlation force	10^{-12} N	-0.585×10^2	1%
The direct electrostatic force	10^{-12} N	-0.596×10^2	0%
The collision force	10^{-12} N	0.106×10^{-2}	1%
The osmotic force	10^{-12} N	0.665×10^1	3%
The total force	10^{-12} N	0.782×10^1	7%
The cell force	10^{-12} N	0.497×10^1	1%
The net macroion force	10^{-12} N	0.286×10^1	8%

the substantial problems in the determination of the polymer chemical potential needed in the application of the insertion technique by simply evaluating the average [Eq. (3.5)] numerically, where the delta function was approximated with a finite size blip. We checked this procedure in the limiting case of no connected counterions and found perfect agreement with the modified insertion technique.

We checked Eq. (3.8) also numerically, see Fig. 2. One can distinguish that F_n of Eq. (3.1) approaches a constant value as the separation between macroions increases. Also one can plot the total force Eq. (3.1) together with its isotropic part F_{cell} [Eq. (3.6)], and verify that they are indistinguishable at large separations between the macroions thus proving the necessity of rescaling embodied in Eq. (3.8). The radius of the simulation cell should be chosen large enough in comparison with the separation between the macroions so that the configuration of the macroions does not perturb the density of the counterions at the cell wall. Figure 2 shows the total force and its isotropic component for two choices of $R_{\text{cell}}=180$ and 240 Å. The total force curves for different cell radii are just displaced in the vertical direction, without any significant changes in their shapes. F_{cell}, on the contrary, is approximately constant for $R_{\text{cell}}=320$ Å, but ceases to remain so for the smaller cell radius. This is understandable since for $R_{\text{cell}}=180$ Å at maximal interaggregate separations the surfaces of the macroions approach prohibitively close to the surface of the cell, locally perturbing the one particle density at the cell surface. It is only above a certain minimal cell radius that F_{cell} actually remains unaffected by the interaggregate separation. One can thus assess the adequacy of the chosen cell radius by monitoring the dependence of the isotropic force component [Eq. (3.6)] on the separation between the macroions.

For all the simulations with simple counterions we verified the constancy of F_{cell} over the whole range of investigated separations between the two spherical macroions.

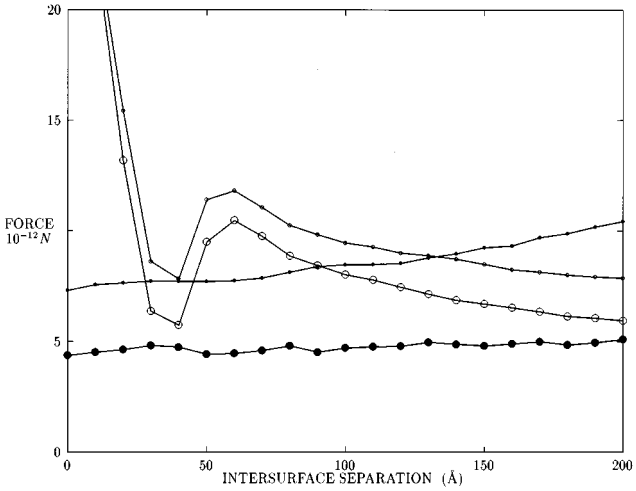

FIG. 2. An illustration of the rescaling [Eq. (3.8)]. The total force F_n (open circles), Eq. (3.2) and the isotropic bulk contribution to the force F_{cell} (filled circles), Eq. (3.7) as functions of the intersurface separation between the two macroions, in the case of a $N=20$ with 40 simple counterions for two cell dimensions, $R_{\text{cell}}=180$ Å (small circles) and $R_{\text{cell}}=320$ Å (large circles). In the case of the large value of R_{cell} F_n approaches a constant value equal to F_{cell} on increase of the intermacroion separation. For the smaller value of R_{cell} the isotropic bulk contribution to the force varies with the separation between the macroions.

V. A SINGLE CHAIN

We first of all analyze the force between two charged spherical aggregates in the presence of a single neutralizing charged chain, see Fig. 3. For a 20-bead chain we see that the shape of the force curve depends on the electrostatic coupling between the chain and the charged aggregates. For sufficiently large surface charge density on the spherical aggregate, however, the general shape of the force curve remains the same. Excluding the region of very small intersurface separations, the force curve displays an attractive regime approximately linear in its dependence on the intersurface separation that ends in a sudden drop of the force to much smaller, but still attractive values. For aggregate radii larger than ≈ 20 Å, the force curve displays no linear attractive regime. At very small separations the picture is somewhat more complicated since the dependence on the aggregate radius is not monotonic. For very small aggregate radii, $R_A=3$ Å, the force at very small separations is large and attractive, while for larger radii, $R_A=10$, 20 Å, it becomes large but repulsive to diminish again as the aggregate radius is increased even further.

The associated changes in the conformation of the chain as exemplified by the mean end–end separation of the polymer (insert of Fig. 3) are revealing. We find that the sudden break in the force curve is invariably accompanied by a major change in the configuration of the polymer chain. This appears to be a salient feature of the polymer mediated interactions and has been stressed in previous work on polymer

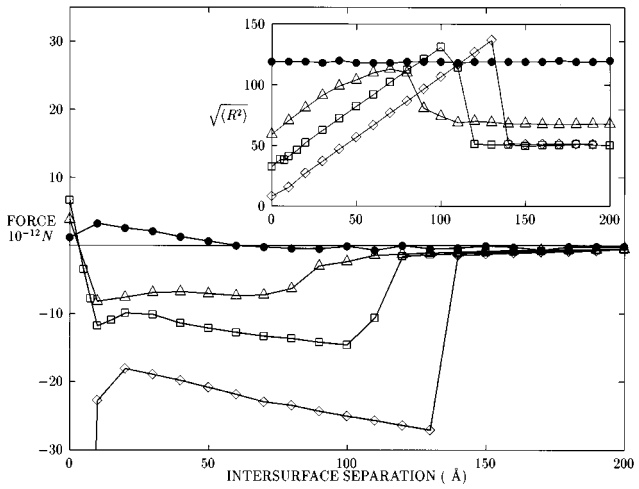

FIG. 3. The net force as a function of the intersurface separation between the macroions for different radii. The length of the chain is 20 beads in all the force curves. The symbols are as follows: $R_A=3$ Å ($\diamond$), $R_A=10$ Å ($\square$), $R_A=20$ Å ($\triangle$), $R_A=100$ Å ($\bullet$). The insert shows the corresponding variations in the mean end–end separation. On this as on all the other figures the intermacroion force is measured in 10^{-12} N.

TABLE II. The breakdown of the total force between two macroions and a neutralizing charged polymeric chain into the constituent components. R_A is the radius of the macroion. The polyelectrolyte chain is 20 beads long, $N=20$, thus giving for the charge on the macroion, $-10e_0$. The different contributions to the total force between the spherical aggregates are defined in Eq. (3.2). The Coulombic part refers to the sum of the correlation term and the direct electrostatic force between the macroions. All force contributions are measured in units of 10^{-12} N.

D (Å)	R_A (Å)	Osmotic	Bridging	Coulombic
	3	2.7	−23.8	−1.0
	10	10.8	−21.2	−1.6
10	20	21.7	−29.7	0
	50	28.6	−33.3	5.9
	100	16.5	−19.0	5.7
	3	2.6	−26.1	0.7
	10	3.5	−18.9	2.0
70	20	4.1	−14.2	2.9
	50	6.2	−11.5	2.7
	100	8.25	−12.5	4.0
	3	0.05	−0.1	−1.4
	10	0.0	−0.0	−1.2
140	20	0.0	−0.0	−1.0
	50	0.8	−1.5	−0.2
	100	2.7	−4.5	1.5

mediated forces in systems with planar symmetry.[9] First of all the mean end–end separation of the 20 - bead polymer indicates that for small electrostatic couplings, i.e., large aggregate radii, the configuration of the chain is unaffected by the presence of external electrostatic fields. Its average dimensions remain practically unaffected by the separation between the aggregates and equal to its value in the absence of any external field, see $R_A=100$ Å in Fig. 3. As the electrostatic coupling is increased the chain becomes severely affected by the presence of the charged aggregates. At small and intermediate interaggregate separations the dimension of the chain scales linearly with $D=|\mathbf{R}_1-\mathbf{R}_2|-2R_A$. This region in the conformational space of the chain coincides with the attractive regime in the force curve. As the separation is increased above a critical value, D_c, depending on the radius of the aggregate, the dimension of the chain is drastically reduced and remains constant if the separation is increased further. A view at the configuration of the system indicates that the chain snaps from a bridging configuration, where it is shared by both aggregates, to a localized configuration where it remains in the vicinity of a single aggregate (see Fig. 1).

A detour regarding nomenclature is in order at this point. We propose to call a chain that has a symmetric monomer density distribution with respect to both aggregates as being *captured* by them.[22] A configuration of the chain, where it embraces both aggregates and is not localized in the vicinity of one of them is thus referred to as *captured* configuration. On the contrary when the monomer distribution is not symmetric with respect to both macroions we refer to the chain as being *localized* in the vicinity of a single macroion (see Fig. 1).

Table II gives the breakdown of the force in Fig. 3 into different components, defined in Eq. (3.2), for three values of the intersurface separation, $D=10,\ 70,\ 140$ Å. First of all we note that at small and intermediate separations, for the very small interaggregate radius, the bridging contribution to the force is overwhelming. For larger radii it is however counteracted by an increasing osmotic force. This is understandable as the electrostatic coupling for small aggregates is largest, giving a low monomer concentration at the midplane. On the other hand, the bridging term, stemming from the stretching of monomer–monomer bonds, is of high strength under such conditions. At even larger radii the Coulombic term contributes significantly to the force, which may become repulsive. At large separations, $D=140$ Å, after the symmetry breaking transition of the monomer density distribution the forces are overall weak, dominated by the Coulombic contribution that derives from the charge reversal on the aggregate onto which the chain finally localizes. The force becomes thus basically a Coulomb attraction between two oppositely charged spheres, decaying as D^{-2}.

In prospect we would like to determine whether the dependence of the force on N, the number of monomers in the polymer chain, can be described in terms of simple scaling laws. Figure 4 presents the force between two $R_A=20$ Å aggregates for different chain lengths, the longest one being $N=100$. We see that for sufficiently large N (actually already for $N\geqslant 20$) the shape of the force curve remains the same if we scale it with respect to the length of the chain. Initially there is a repulsive regime dominated by the osmotic contribution, that gives way to a bridging dominated attraction linear in the separation. This regime is terminated abruptly after the captured chain makes its symmetry breaking leap to one of the aggregates. Notably at larger chain lengths (and thus higher aggregate charge) there is an additional regime between osmotic repulsion at small separations and bridging attraction at larger separations, where the force is still attrac-

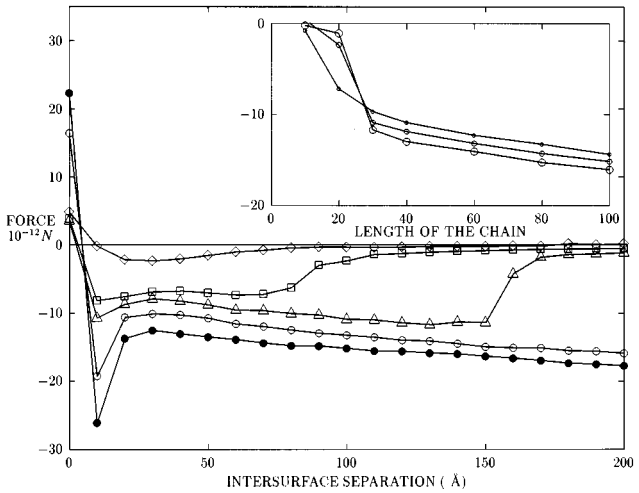

FIG. 4. The net force as a function of separation with variable length of the neutralizing polymer chain. The radius of the macroion is $R_A=20$ Å. The lengths of the neutralizing polymer chain are: $N=10$ ($\diamond$), $N=20$ ($\square$), $N=30$ ($\triangle$), $N=60$ ($\bigcirc$), $N=100$ ($\bullet$). The insert shows the scaling of the force with the length of the chain at separations: $D=70$ Å (small open circle), $D=100$ Å (medium open circle), and $D=130$ Å (large open circle).

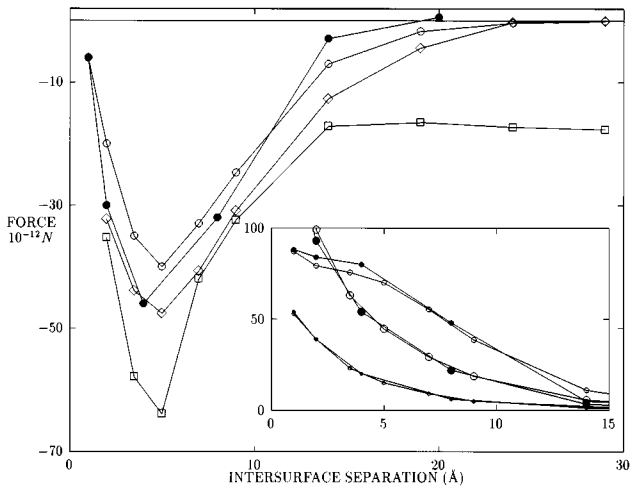

FIG. 5. Forces between two uniformly charged spherical macroions with radius $R_A=18$ Å with terminally attached ($\bigcirc$) and unattached ($\bullet$) chains. The number of chains is 12. In the attached case each of the chains is composed of ten monomers with an additional link to the surface of the macroion. The unattached chains are composed of ten monomers without any force links to the surface. The insert shows the breakdown of the total force into an ideal contribution (open and filled large circles), minus harmonic contribution (medium open and filled circles) and minus electrostatic correlation forces (small open and filled circles). The other force curves represent: four chains 30 beads long ($\diamond$) and three chains 40 beads long ($\square$), all unattached to the surface of the macroion.

tive but larger than the simple scaling law would have us predict. This extra attraction at high electrostatic coupling (cf. Fig. 4) is also due to bridging, but of the same kind as found in a planar system.[6] In this case the force is strong but short ranged and is due to several bonds stretching across the midplane. As the separation increases the energy for such a configuration increases rapidly, and the chain becomes captured with only one bond across the midplane.

The dependence of the force on the length of the chain gives us some insight into the scaling properties of the force. Clearly for a long enough chain the force scales linearly with N at most of the separations, while at the same time it remains also an approximately linear function of D for separations smaller than the capture distance. We can thus make the following empirical conjecture: at separations where the chain is captured the form of the polymer mediated force can be represented approximately as

$$f\sim -a\left(\frac{D}{\ell}+bN^{\rho}\right), \tag{5.1}$$

where $\ell^2=3kT/\mathscr{K}_F$, a and b depend on R_A, while $\rho\sim 1$. At larger separations, following the symmetry breaking leap of the chain and its localization, we would have on the other hand

$$f\sim -\frac{e^2}{D^2}, \tag{5.2}$$

a force which, apart from the sign, would be about the same as the repulsive force between bare aggregates.

VI. GRAFTED AND FREE CHAINS

We now consider a system with two macroions and several polyelectrolyte chains, which are grafted with one end to either of the macroions. It has been observed that this system behaves qualitatively as a planar system, although with a slightly weaker and more short ranged bridging attraction.[17]

First of all we note that the constraints brought in by grafting one end of the chains to a surface of the macroion do not act drastically on the interaction, see Fig. 5. A general observation is, however, that as long as the total number of chains is even, enabling them to partition equally among the two macroions to neutralize their charge, the magnitude of the overall polymer mediated force changes only moderately with length or number of the chains.

If on the other side the number of chains is odd, meaning that there is no simple partitioning of chains equally among the two macroions, the ensuing force looks rather different. At intermediate separations the force does not approach zero as in the case of equal partitioning of the chains among the two macroions, but remains attractive, scaling approximately linearly with D. In its overall form the force in this regime looks like the force in the captured regime, signifying that it mainly stems from the bridging contribution of a single chain that is trying to neutralize both macroions simultaneously. Also the force in the case of an odd number of chains looks approximately like a superposition of a short range bridging force, extending to about 15 Å, and a long range one, extending to the interaggregate separations of the order of the unperturbed length of the chain.

Despite the limitation of the cell model there are several general conclusions that we can extract: whenever the chains can partition equally among the macroions, meaning that the number of chains neutralizing each of the two macroions is

the same, the electrostatic attraction forces them to reside close to the respective adsorbing surfaces. As the chain entropy is rather low in this condition, the chain can gain additional entropy by bridging from one charged macroion to the other one. As the electrostatic potential is very high in the region between the macroions the bridging can only involve one or two monomers, with most of the chain remaining in close proximity of the macroion surfaces. The overall dependence of the force on the length of the polyelectrolyte chains should be marginal in this case. The attraction will be strong but short ranged, on the order of the monomer–monomer separation. Most of the bridging attraction in this case comes from the stretching of a small number of bonds across the midaggregate plane and is entropy driven. With an odd number of chains one of them will eventually have to compensate charges on both of the macroions. This will lead to a situation close to the capturing of the chain described in the previous section, where most of the attraction is derived from the electrostatic interaction energy between the bridging chain and the two macroions. And indeed, see Fig. 5, with an odd number of chains we invariably end up with a long range force going approximately linearly with separation until the chain localizes to one macroion. The dependence of the force on the length of the chain is quite pronounced in this case. The breakdown of the force into its constituents also indicates that the terms seriously affected as we go from even to odd number of chains are the (dominating) bridging term and the osmotic term which become long range for an odd number of chains. We would be able to observe a similar effect also with a larger number of interacting macroions, where a long range bridging force would develop whenever the number of chains would not be divisible by the number of macroions.

If we want to draw a lesson for the possible experimental situations we have to conclude that whenever the concentration of the chains is small compared to the concentration of the macroions, the chains will try to compensate the charge on several macroions conferring to them at the same time a long range bridging attraction. If on the other hand the concentration of the polymer is large compared to the concentration of macroions, each chain can remain in the vicinity of a single macroion, making the long range bridging unprobable. The short range bridging would however remain intact and the macroions would behave as sticky spheres.

VII. POLYCOUNTERIONS AND SIMPLE COUNTERIONS

We now generalize our model system by adding simple counterions to the already present polycounterions. The dependence of the interaggregate force on the amount of simple counterions, N_C, present in a cell with $R_{\text{cell}}=240$ Å is shown in Fig. 6. For $N=30$, we analyzed four cases: no additional counterions, the number of counterions is half the number of beads in the chain, the number of counterions is equal to the number of beads in the chain and the number of counterions is twice the number of beads in the chain—with the assumption of the overall electroneutrality. With $N_C=15$ we see that the capture transition occurs at basically unchanged value of D, set by the value of N. The magnitude of the force is, however, increased. The dependence of the force on D is of the same type as in the absence of counterions, with a long range attractive regime after the chain is localized, where the force goes as D^{-2}. If we make $N_C=30$, we first of all note that the capture separation has decreased. Below the capture separation the force again shows all the characteristics of the long range bridging observed without any counterions. Above the capture separation the force is essentially zero. Increasing the amount of counterions even more makes the capture separation move further in, while the force in the captured regime remains attractive only at a very narrow range (if at all). After the chain snaps to one of the aggregates the force turns repulsive. Actually the repulsive branch of the force is hardly distinguishable from the force acting in the presence of simple counterions only, which is just the double-layer force due to the inhomogeneous distribution of the counterions. We thus come all the way from the polymer dominated to the counterion dominated interaggregate force. Note that for large amounts of the counterions the force could be described as being due to ''sticky'' spheres—it is repulsive for large separations but has an attractive hump, extending over very small separations where it is attractive and reasonably large.

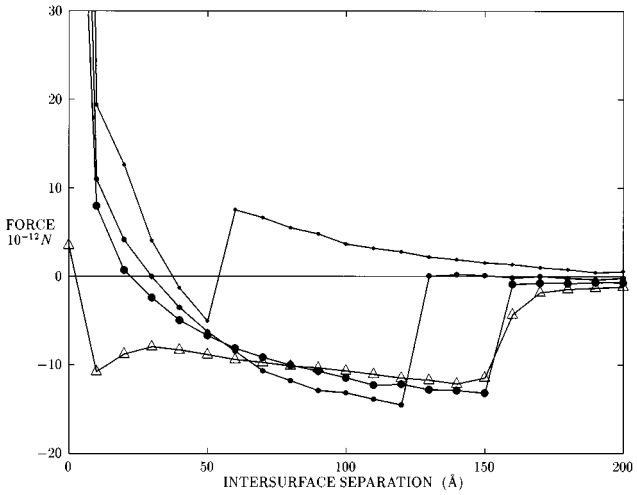

FIG. 6. Net forces (see the main text) between macroions in the presence of polyelectrolyte and simple counterions. Chain with $N=30$ and no counterions (△), with 15 counterions (large filled circles), with 30 counterions (medium filled circles), with 60 counterions (small filled circles). The radius of the cell was taken as $R_{\text{cell}}=240$ Å.

The breakdown of the total force into its components, see Table III, might give us a clearer idea on the role played by the polymer and the counterions. We note that the larger the number of counterions, the larger is their concentration at the midplane and the larger is their osmotic contribution to the force. When the bridging contribution is not important, then the interaction may be qualitatively described as a double-layer type repulsion. The osmotic contribution of the polymer beads does not change drastically with the amount of simple counterions present as long as the chain is captured by both macroions. After that it is essentially zero. The behavior of the bridging contribution to the total force indicates

TABLE III. The breakdown of the force between two spherical aggregates $R_A=20$ Å, for different chain lengths and different amount of simple counterions. The comparison is done at two separations, $D=60$ Å and $D=120$ Å. In the captions the different contributions refer to the different terms in the force balance equation, Eq. (3.2). The Coulombic part refers to the sum of the correlation term and the direct electrostatic force between the macroions while the osmotic term is broken down into a separate polymer and counterion contribution. All the force contributions are measured in units of 10^{-12} N. The radius of the cell was taken as $R_{\text{cell}}=240$ Å.

D (Å)	N	N_C	Osmotic (Pol.)	Osmotic (Cou.)	Bridging	Coulombic	-Isotropic
	30	60	0.04	5.25	−0.06	3.38	−3.18
60	30	30	3.40	3.52	−19.47	2.32	−2.55
	30	15	3.79	1.85	−17.99	1.91	−1.66
	30		4.38		−16.60	2.77	
	30	60	0.07	4.20	−0.09	0.87	−3.27
120	30	30	2.78	2.90	−22.77	1.41	−2.24
	30	15	3.12	1.65	−20.63	1.90	−1.37
	30		3.65		−18.40	3.37	

that addition of counterions makes the bridging term larger if the chain is captured, see the behavior of this component for $N=30$ chain at both separations in Table III. This is not really surprising, since the increasing counterion concentration also implies an increase of the macroion charges. Therefore it is energetically more convenient for the polymer beads to move more towards the oppositely charged aggregate surfaces. This leads to more pronounced stretching of the chain and the bridging term increases. This trend is followed on addition of counterions up to a point, where the stretching of the chain is energetically too costly and the chain collapses to one of the aggregates. The same reasoning applies to a certain number of counterions while varying the separation leads to the conclusion that the symmetry breaking transition from the captured state of the chain should occur at smaller interaggregate separations in the presence of additional counterions. The sum of the correlation and the direct electrostatic interactions between the aggregates does not show any drastic changes due to the presence of monovalent counterions, while the isotropic contribution, or equivalently the bulk pressure in the cell increases with increasing amount of counterions in the cell.

The effect of the simple counterions on the force between the macroions, if the charge on the macroions is kept fixed is shown in Fig. 7. It is obvious that the upper bound of the force is given by the double-layer repulsion where all the countercharge is in the form of the simple counterions. On the contrary, the lower bound of the force is not given by the case where all the countercharge is in the polymer chain, as the simple counterions effect is not additive. The exchange of monomer charges by simple counterions may under some circumstances lead to an increased bridging attraction, but it will simultaneously reduce its range.

VIII. DISCUSSION

It is difficult to rationalize all the findings on the polyelectrolyte mediated force in terms of a comprehensive theoretical model. There are, however, some partial results that one can derive from simple theory that shed some light on the characteristics and the mere existence of the long range bridging force. It will be our purpose in what follows to establish at least partial connections between the MC results and simple theory.

A. Mean-field approximation

We present a simple mean-field analysis of the polyelectrolyte in an external electrostatic field of two oppositely charged macroions. For the sake of simplicity we shall ignore the finite extension of the macroions and shall treat them as point sources ($R_A=0$). For a polyelectrolye chain N beads long described by the Hamiltonian equation (2.1) but without any hard-core interactions, the number of configurations with fixed ends at $\mathbf{r}$ and $\mathbf{r}'$, respectively, $\mathcal{G}(\mathbf{r},\mathbf{r}';N)$, is given as

$$\mathcal{G}(\mathbf{r},\mathbf{r}';N)=\sum_i e^{-E_iN}\Psi_i(\mathbf{r})\Psi_i(\mathbf{r}'), \tag{8.1}$$

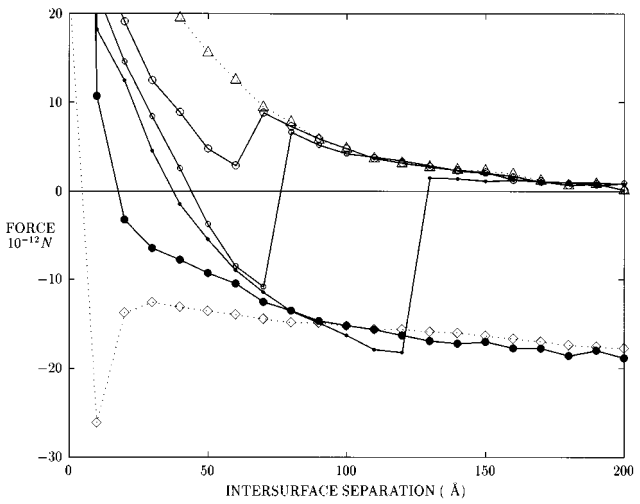

FIG. 7. Polymer chain of different length plus additional simple counterions. The total number of particles is being held constant at 100. $N=20$ (large open circles), $N=30$ (medium open circles), $N=40$ (small filled circles), $N=80$ (large filled circles), $N=100$, i.e., no simple counterions (lower dotted line), and $N=0$, just simple counterions (upper dotted line).

where the eigenfunctions are solutions of the Schrödinger equation[23]

$$\left[-\frac{\ell^2}{6}\nabla^2-\mathscr{U}_C(|\mathbf{R}_1-\mathbf{r}|)-\mathscr{U}_C(|\mathbf{R}_2-\mathbf{r}|)\right]\Psi_i(\mathbf{r})=E_i\Psi_i(\mathbf{r}), \tag{8.2}$$

where we introduced $\ell^2=3kT/\mathscr{K}_F$ and described the chain with a continuous version of the bond potential [Eq. (2.21)].

A lowest order solution of the above equation is constructed from an analogous quantum mechanical problem,[24] that gives to the lowest order in the inverse separation between the two macroions, $|\mathbf{R}_1-\mathbf{R}_2|=D$, the following result:

$$\Delta E_0(D)\cong-\frac{\ell^2}{6\lambda_E^3}\int_{(S)}d^2\mathbf{r}\Psi_0(\mathbf{r})\frac{\partial}{\partial\mathbf{n}}\Psi_0(\mathbf{r}), \tag{8.3}$$

where λ_E measures the length scale and is given by $\lambda_E=\ell^2/3N\lambda_B=\ell^2 4\pi\epsilon\epsilon_0 kT/3Ne_0^2$, with λ_B being the Bjerrum length, while $\Delta E_0(D)$ is the change in the eigenenergy when the second macroion is brought to a separation D and $\mathbf{n}$ is the normal to the integration plane S that coincides with the midplane between the two macroions. $\Psi_0(\mathbf{r})$ is the ground state solution of Eq. (8.2) that one approximates with $\Psi_0(\mathbf{r})\cong a(\mathbf{r}-\mathbf{R}_1,\mathbf{r}-\mathbf{R}_2)e^{-|\mathbf{R}_1-\mathbf{r}|/\lambda_E}$, or with an analogous expression centered on $\mathbf{R}_2$. This *ansatz* stems from the form of the eigenfunction for a single macroion, when $\lim_{D\to\infty}a(\mathbf{r}-\mathbf{R}_1,\mathbf{r}-\mathbf{R}_2)$ is actually a constant. By inserting this *ansatz* back into Eq. (8.2) one can determine the form of $a(\mathbf{r}-\mathbf{R}_1,\mathbf{r}-\mathbf{R}_2)$. The function $a(\mathbf{r}-\mathbf{R}_1,\mathbf{r}-\mathbf{R}_2)$ is evaluated approximately only in the region close to the axis connecting the two macroions, what finally gives the approximate form for the change in the free energy of the system on approach of the second macroion:[24]

$$\begin{aligned}F&=-kT\int\int d^3\mathbf{r}\,d^3\mathbf{r}'\mathscr{G}(\mathbf{r},\mathbf{r}';N)\\&\cong kT\Delta E_0(D)N\sim-\frac{36}{e}kT\frac{N^4\lambda_B^3}{\ell^3}De^{-\frac{3N\lambda_B}{\ell^2}D},\end{aligned} \tag{8.4}$$

where F is the free energy of the chain as a function of D. Even in this very simplified mean-field analysis one is thus able to demonstrate that a polyelectrolyte chain in an attractive field of two oppositely charged macroions confers an effective attraction to them. We can derive the following approximate form of the force:

$$f=-\frac{\partial F}{\partial D}\sim-kTN^5\lambda_B^4De^{-\frac{3N\lambda_B}{\ell^2}D}. \tag{8.5}$$

The major drawback of the above analysis is that it does not include the self-interaction of the chain what leads to the wrong scaling of the force with respect to N. Nevertheless for short chains where the effect of the self-interactions is small the above theory should qualitatively describe the attractive force. There is no simple way to approach the effects of self-interactions on this level of the theory and we revert to alternative approaches.

B. Variational approach

One way to include the electrostatic self-interactions along the chain into the picture would be to employ a variational principle on an easy to treat *ansatz*. This has been accomplished recently for a generalized quadratic variational Hamiltonian.[25] The configurational properties of the electrostatically self-interacting chain obtained variationaly were found to be in very good aggreement with simulation results.[26]

With a quadratic *ansatz* the configurational properties of the chain with a microscopic Hamiltonian [Eq. (2.1)] (but with the hard-core repulsion omitted) are deduced from a ''chain smeared'' configurational energy of the form[25]

$$\begin{aligned}W(\mathbf{r}_0)=&\int d^3\mathbf{r}\mathscr{U}_C(|\mathbf{R}_1-\mathbf{r}|)\rho_{a^2}(\mathbf{r},\mathbf{r}_0)\\&+\int d^3\mathbf{r}\mathscr{U}_C(|\mathbf{R}_2-\mathbf{r}|)\rho_{a^2}(\mathbf{r},\mathbf{r}_0)\\&+\frac{1}{2}\int\int d^3\mathbf{r}\,d^3\mathbf{r}'\rho_{a^2}(\mathbf{r},\mathbf{r}_0)u_C(|\mathbf{r}-\mathbf{r}'|)\rho_{a^2}(\mathbf{r}',\mathbf{r}_0),\end{aligned} \tag{8.6}$$

where $\rho_{a^2}(\mathbf{r}',\mathbf{r}_0)$ is a Gaussian distribution of chain segments around the center of mass of the chain, $\mathbf{r}_0$, with a variance $a^2(\mathbf{r}_0)$, which is determined variationally.[25] Setting $a^2(\mathbf{r}_0)=(\ell^2/3\zeta_0)\mathscr{L}(\zeta_0N/2)$, where $\mathscr{L}(x)$ is the Langevin function, one obtains ζ_0 as a solution of the Euler–Lagrange equation in the form

$$\frac{3}{2}kT\zeta_0^2(\mathbf{r}_0)N=\frac{\partial}{\partial a^2}W(\mathbf{r}_0). \tag{8.7}$$

Once the variational equation is solved, the free energy is obtained as a complicated integral over $\mathbf{r}_0$ and is a function of the chain length and the magnitude of the macroion charges at $\mathbf{R}_1$ and $\mathbf{R}_2$.

In the case of two equally charged macroions [with charge $-(1/2)Ne_0$)] separated by $|\mathbf{R}_1-\mathbf{R}_2|=D$ (the macroions are again treated as point sources), we obtained explicit expressions for the free energy in two limiting cases.[25] If the separation between macroions is large compared to the length of the chain, the free energy has the approximate form

$$F\cong kT\frac{\ell^2}{2}\left(\frac{N}{a^2}\right)+\frac{e_0^2N^2(1-\sqrt{2})}{\epsilon\epsilon_0(4\pi)^{3/2}a}-\frac{e_0^2(N^2/4)}{4\pi\epsilon\epsilon_0D}+\dots. \tag{8.8}$$

In this limiting case the chain is localized in the vicinity of **one** of the two macroions with the mean end to end separation equal to $\sqrt{\mathscr{R}^2}=$const, being independent of N. The density distribution of the chain has in this case a spontaneously broken symmetry. Furthermore the interaction between the two charges is the same as if the polymer was absent, but with a sign reversed (attraction instead of repulsion).

In the opposite limit the free energy is obtained in the form

$$F\cong\frac{e_0^2(N^2/4)}{4\pi\epsilon\epsilon_0D}+kT\frac{\ell^2}{2}\left(\frac{N}{a^2}\right)\left[-1+\frac{2^{3/2}}{2^{3/2}-1}\frac{D^2}{3a^2}+\dots\right], \tag{8.9}$$

where except for the very small separations the second term, providing an attractive force linear in the separation between the macroions, dominates. The polymer density distribution is in this case symmetric with respect to both external charges. One should note here that the dependence on the chain length in Eq. (8.9) is very different from the case of an ideal chain under external traction though the D dependence is quadratic in both cases.

The general picture that emerges from the variational calculation thus supports a polyelectrolyte mediated attraction between the two external charges at small separations, with a symmetric distribution of the polymer segments in the space between the charges, while for separations larger than $D \cong N\ell$ there is a symmetry breaking transition in the polymer density distribution leading to a charge reversal on one of the external charges and the force becomes ordinary electrostatic attraction.

C. Scaling analysis

The mean-field analysis given previously could be criticized from the standpoint of not having the intrachain interactions properly included in the calculation while it can be shown that the variational approach is strictly valid only in the limit of short chains.[27] However, there is yet another revealing way, not hampered by the above limitations, to assess the qualitative effects of the self-interactions along the polymer chain on the interactions mediated by it, offered by the scaling arguments. In the most simple scaling analysis the free energy for a chain captured by the two aggregates has the form

$$F \sim aM^2 - 2bNM + kT\left(\frac{D}{\ell}\right)^{1/1-\alpha}(N-M)^{-\alpha/1-\alpha}. \tag{8.10}$$

The first term corresponds to Coulombic self-interaction of the M beads of the whole chain that are adsorbed to the two oppositely charged aggregates, the second one to the Coulombic interaction between the adsorbed parts of the chain and the charges on the aggregates (the system is overall electroneutral), while the last one describes the stretching of the part of the chain that occupies the space between the aggregates and contains also the self-energy of the stretched part of the chain.[22] α is the usual exponent associated with the swelling of the chain, $\sqrt{\mathscr{R}^2} \sim N^{\alpha}$. While writing down Eq. (8.10) we disregarded the detailed structure of the adsorption layer, assuming that all the adsorbed monomers are located right at the surface, and used only the roughest scaling forms for the different parts of the free energy.[28]

In order to get the equilibrium force we first of all have to minimize F with respect to M, i.e.

$$\frac{\partial F}{\partial M} = 2aM - 2bN + kT\,\frac{\alpha}{1-\alpha}\left(\frac{D}{\ell}\right)^{1/1-\alpha}(N-M)^{-1/1-\alpha} = 0. \tag{8.11}$$

The general form of this minimization condition is untractable, but there are revealing limiting cases that yield to simple analysis. For $M < N$ at sufficiently large separations we obtain approximately

$$M \sim N\left[1 - g_0^{1-\alpha}N^{\alpha-2}\left(\frac{D}{\ell}\right)\right], \tag{8.12}$$

where we introduced $g_0 = kT\alpha/(1-\alpha)2b$. The ensuing force assumes in this limit the approximate form

$$f = -\frac{\partial F}{\partial D} \sim -2a\,\frac{g_0^{2(1-\alpha)}N^{2(\alpha-1)}}{\ell^2}\,D - kT\,\frac{g_0^{-\alpha}N^{\alpha}}{(1-\alpha)\ell}\left(1 - \frac{a}{b}\,\alpha\right). \tag{8.13}$$

Expression (8.13) for the force describes a long range attraction, extending over separations of the order of the length of the chain, terminating abruptly at $D = D_c \sim \ell N^{2-\alpha} g_0^{\alpha-1}$, where the symmetry breaking transition occurs. The scaling of the attractive force with D and N is completely consistent with simulation results [Eq. (5.1)] for the electrostatically stiffened chain with $\alpha \cong 1$. At $D = D_c$, the attractive force will cease to exist and the chain will make a symmetry breaking jump to one of the spheres, quite in a similar vain as in the more simple planar uncharged case[22] where the force in the captured regime is a constant and where the adsorbing potential is short ranged.

The presence of attractive bridging interactions appears to be a salient feature of the polyelectrolyte colloid systems. There are however at least two distinct ways how polyelectrolyte bridging can confer attraction between oppositely charged macromolecular aggregates. First of all one has the *entropic* bridging which stems from the chain configurations spanning the interaggregate region by means of which the chains gain substantial entropy. This attraction is strong but of short range, spanning at most the region of a few monomer–monomer separations. It operates in planar systems where the charges on the bounding surfaces create no electrostatic potential. The *energetic* bridging operates between charged spherical aggregates (or any other nonplanar geometries for that matter) that can create large intervening electrostatic potentials. It does not stem from the enhanced entropy of the bridging chains but rather from the energetics of the chain–aggregate interactions right at the aggregate surface. This type of bridging force is much longer ranged than the *entropic* bridging and can be orders of magnitude larger than the van der Waals force.

The existence of the long range bridging force has been clearly demonstrated through simulations as well as theoretical calculations. The model situation envisioned in both was of course quite simplified. As already stated we did not take into account the many-body effects due to the existence of other macroions in solutions. Also we presumed that the energy scale of polyelectrolyte–macroion interaction is much lower than the energy scale of macroion deformations. In case of e.g., DNA–cationic liposome interaction[12] we know that the complexation induced by DNA bridging also eventually leads to deformation and rupture of the liposomes. These situations are well beyond the level of understanding of polyelectrolyte bridging phenomena promoted in this contribution. Nevertheless we believe that a closer permeation of

liquid state as well as polymer physics approaches should provide additional insight into the complex set of phenomena involving polyelectrolyte bridging.

ACKNOWLEDGMENTS

One of the authors (R.P.) would like to thank the Swedish Research Council for the research fellowship that made his stay at the Chemical Center of the University of Lund, where this work was performed, possible. He would also like to acknowledge a travel grant from the Ministry of Science and Technology of Slovenia.

[1] J. Israelachvili, *Intermolecular and Surface Forces* (Academic, London, 1992).
[2] L. Guldbrand, B. Jönsson, H. Wennerström, and P. Linse, J. Chem. Phys. **80**, 2221 (1984).
[3] R. Kjellander and S. Marčelja, J. Chem. Phys. **82**, 2122 (1985).
[4] V. Shubin and P. Kékicheff, J. Chem. Phys. **99**, 6098 (1993).
[5] D. H. Napper, *Polymeric Stabilization of Colloid Dispersions* (Academic, New York, 1983).
[6] T. Åkesson, C. Woodward, and B. Jönsson, J. Chem. Phys. **91**, 2461 (1989).
[7] M. Dahlgren, Å. Waltermo, E. Blomberg, P. Claesson, L. Sjöström, T. Åkesson, and B. Jönsson, J. Phys. Chem. **97**, 11 769 (1994).
[8] S. Miklavic, C. E. Woodward, B. Jönsson, and T. Åkesson, Macromolecules **23**, 4149 (1990).
[9] R. Podgornik, J. Phys. Chem. **96**, 884 (1992).
[10] D. W. McQuigg, J. I. Kaplan, and P. I. Dubin, J. Phys. Chem. **96**, 1973 (1992); S. Wall, P. Samuelsson, G. Degerman, P. Skoglund, and A. Samuelsson, J. Colloid Interface Sci. **151**, 178 (1992).
[11] B. Cabane and R. Duplessix, Colloid Surf. **13**, 19 (1985).
[12] R. Ghirlando, Ph.D. thesis, The Weizmann Institute of Science (1991); H. Gershon, R. Ghirlando, S. B. Guttman, and A. Minsky, Biochemistry **32**, 7143 (1993).
[13] T. L. Hill, *Statistical Mechanics* (Addison-Wesley, Reading, MA, 1960).
[14] R. Podgornik and B. Jönsson, Europhys. Lett. **24**, 501 (1993).
[15] A. Baumgärtner, in *Applications of the Monte Carlo Method in Statistical Physics*, 2nd ed., edited by K. Binder, Topics Curr. Phys. (Springer, Berlin, 1987) Vol. 36, Chap. 5.
[16] H. Wennerström, B. Jönsson, and P. Linse, J. Chem. Phys. **76**, 4665 (1982)-
[17] M. K. Granfeldt, B. Jönsson, and C. E. Woodward, J. Phys. Chem. **95**, 4819 (1991).
[18] R. Lovett and M. Baus, J. Chem. Phys. **97**, 8596 (1992).
[19] J. P. Valleau, R. Ivkov, and G. M. Torrie, J. Chem. Phys. **95**, 520 (1991).
[20] N. A. Metropolis, A. W. Rosenbluth, M. N. Rosenbluth, A. Teller, and E. Teller, J. Chem. Phys. **21**, 1087 (1953).
[21] B. Svensson, T. Åkesson, and C. Woodward, J. Chem. Phys. **95**, 2717 (1991).
[22] A. Johner, E. Bauchaud, and M. Daoud, J. Phys. France **51**, 495 (1990).
[23] K. Freed, *Renormalization Group Theory of Macromolecules* (Wiley, New York, 1987).
[24] L. D. Landau and E. M. Lifshitz, *Quantum Mechanics* (Pergamon, London, 1954).
[25] R. Podgornik, J. Chem. Phys. **99**, 7221 (1993).
[26] B. Jönsson, C. Peterson, and B. Söderberg, Phys. Rev. Lett. **71**, 376 (1993).
[27] H. Kleinert, *Path Integrals in Quantum Mechanics, Statistics and Polymer Physics* (World Scientific, Singapore, 1990).
[28] P.-G. de Gennes, *Scaling Concepts in Polymer Physics* (Cornell University, Ithaca, 1979).